Planetary and Space Science ▮ (▮▮▮▮) ▮▮▮–▮▮▮

Contents lists available at ScienceDirect

Planetary and Space Science

journal homepage: www.elsevier.com/locate/pss

Surface waves on Saturn's dawn flank magnetopause driven by the Kelvin–Helmholtz instability

A. Masters [a,*], N. Achilleos [b], C. Bertucci [a,c], M.K. Dougherty [a], S.J. Kanani [d,e], C.S. Arridge [d,e], H.J. McAndrews [f], A.J. Coates [d,e]

[a] Space and Atmospheric Physics Group, The Blackett Laboratory, Imperial College London, Prince Consort Road, London SW7 2AZ, UK
[b] Atmospheric Physics Laboratory, Department of Physics and Astronomy, University College London, Gower Street WC1E 6BT, UK
[c] Institute for Astronomy and Space Physics, PO Box 67–Suc. 28, C1428ZAA Buenos Aires, Argentina
[d] Mullard Space Science Laboratory, Department of Space and Climate Physics, University College London, Holmbury St. Mary, Dorking, Surrey RH5 6NT, UK
[e] Centre for Planetary Sciences, University College London, London WC1E 6BT, UK
[f] Space Science and Applications, Los Alamos National Laboratory, Los Alamos, NM 87545, USA

ARTICLE INFO

Article history:
Received 14 November 2008
Received in revised form
17 February 2009
Accepted 25 February 2009

Keywords:
Saturn
Magnetosphere
Magnetopause
Waves
Kelvin–Helmholtz instability

ABSTRACT

Crossings of Saturn's magnetopause made by the Cassini spacecraft on 12, 13 and 17 March 2006 are analysed. During this period Cassini's trajectory was approximately parallel to the magnetopause boundary given by a model of the surface. Magnetic field and electron data are used to identify excursions into the magnetosheath bounded by crossings of the magnetopause current layer. Minimum variance analysis of the magnetic field vector measurements is used to determine the normal to the boundary for each crossing. The normals corresponding to the crossings oscillate about an average orientation that is consistent with the unperturbed normal predicted by the surface model. This reveals the presence of regular boundary waves with a direction of propagation found to be within 24° of Saturn's rotational equator. Two categories of boundary wave are identified: the first with a period of the order of hours, and the second with a period of 45 ± 9 min. Based on the propagation direction and a comparison of magnetospheric and magnetosheath magnetic fields, we conclude that both types of wave were driven by the Kelvin–Helmholtz instability. The observed boundary perturbations are consistent with a superposition of different types of surface wave activity.

1. Introduction

The dynamics of planetary magnetopauses has been a topic of intense research for many years; the existence of a magnetopause current sheet separating solar wind and planetary magnetic fields was first proposed by Chapman and Ferraro (1931). This initial concept of a 'closed' magnetosphere was then revolutionised by Dungey (1961) who suggested an 'open' magnetosphere as a result of magnetic reconnection. Earth's magnetopause has been extensively studied since the beginning of the space age using in situ observations (see the review by de Keyser et al., 2005) that have revealed the complicated structure of the boundary, and have provided the basis for our understanding of the stability of planetary magnetopauses in general.

The dynamics of Earth's magnetopause include global expansion and contraction, principally controlled by variations in the solar wind dynamic pressure (e.g. Sibeck et al., 1991); transient episodes known as flux transfer events (FTEs), where magnetospheric flux tubes are ripped off due to sporadic magnetic reconnection with the interplanetary magnetic field (IMF) (Russell and Elphic, 1978, 1979); erosion of the dayside magnetopause, also caused by reconnection (Holzer and Slavin, 1978); and surface waves (Aubry et al., 1971; Lepping and Burlaga, 1979; Chen and Kivelson, 1993; Seon et al., 1995). The driving mechanism of the surface waves has been the subject of much debate; Song et al. (1988) and Sibeck (1990) both suggested that they could be the result of solar wind dynamic pressure fluctuations, and Song et al. (1988) also proposed that they could be caused by reconnection-related phenomena.

The possibility that a planetary magnetopause boundary could become Kelvin–Helmholtz (K–H) unstable was first suggested by Dungey (1955). The K–H instability grows at the interface between two fluids under the appropriate conditions and can manifest itself in the form of boundary waves. Conditions are favourable for the growth of the K–H instability when there is an adequately strong flow velocity shear across the boundary. The kinetic energy of this velocity shear is the source of free energy that drives the instability. The magnetopause K–H instability

* Corresponding author. Tel.: +44 2075947766; fax: +44 2075947772.
E-mail address: adam.masters02@imperial.ac.uk (A. Masters).

0032-0633/$ - see front matter © 2009 Elsevier Ltd. All rights reserved.
doi:10.1016/j.pss.2009.02.010

problem has been investigated by many authors using both a theoretical approach (Fejer, 1964; Sen, 1963, 1965; Southwood, 1968; Pu and Kivelson, 1983a, 1983b; Kivelson and Pu, 1984) and simulations (e.g. Nykyri and Otto, 2001, 2004). Ogilvie and Fitzenreiter (1989) used observations made by the ISEE 1 spacecraft to assess the K–H stability at Earth's magnetopause and inner boundary layer and concluded that the magnetopause itself is generally stable, although the inner boundary layer is often unstable.

Compared to the initial discussion of the problem in the literature, strong observational evidence for the K–H instability at Earth's magnetopause has only been presented recently. In its linear phase the K–H instability generates surface waves; however, when the instability enters its nonlinear phase the waves evolve into 'rolled-up' vortices. Fairfield et al. (2000) argued that multiple magnetopause crossings made by the Geotail spacecraft were due to K–H vortices moving past the spacecraft, before Hasegawa et al. (2004) used the four Cluster spacecraft to unambiguously identify vortices on the dusk flank. The identification of such structures provides conclusive evidence of the instability operating at the terrestrial magnetopause. The possibility that K–H vortices can promote magnetic reconnection has also been discussed (Nikutowski et al., 2002; Nykyri et al., 2006).

In contrast to the terrestrial magnetosphere, Saturn's magnetosphere has only been explored by four spacecraft. Pioneer 11 (Acuña and Ness, 1980; Smith et al., 1980), Voyager 1 (Stone and Miner, 1981) and Voyager 2 (Stone and Miner, 1982) flew by the planet in 1979, 1980 and 1981, respectively, whereas Cassini has been orbiting Saturn since July 2004. The dominant plasma motion within the kronian magnetosphere is (sub)corotation with the planet (Eviatar and Richardson, 1986). This motion results in a strong velocity shear at the dawn flank of the magnetopause (see the review by Lepping, 1992) since at this location the magnetosheath flow and the subcorotating magnetospheric flow are approximately anti-parallel. By contrast, on the dusk flank the flows on either side of the boundary are approximately parallel, resulting in a less dramatic flow velocity shear across the interface.

The K–H instability at Saturn's magnetopause was first discussed by Lepping et al. (1981) who used magnetopause crossings made by Voyager 1 during its inbound leg to identify boundary waves, which they concluded could have been driven by the K–H instability. Pu and Kivelson (1984) then used a theoretical approach to demonstrate that the dawn flank is generally K–H unstable and the properties of their predicted waves were in good agreement with those identified by Lepping et al. (1981). The K–H stability of Saturn's magnetopause was evaluated as a function of Saturn local time by Galopeau et al. (1995), who showed that there is a dawn–dusk asymmetry in the stability of Saturn's dayside, equatorial magnetopause due to the differences in flow shear. They found that the dawn flank is generally K–H unstable whereas the dusk flank is generally K–H stable. Simulation results also suggest that Saturn's magnetopause is unstable to the growth of boundary waves. Fukazawa et al. (2007) carried out a global magnetohydrodynamic simulation of Saturn's magnetosphere and found that vortices formed on the dayside magnetopause before propagating tailward, principally on the dawn flank but also on the dusk flank.

During the initial phase of Cassini's orbital tour of the kronian system the spacecraft explored the dawn sector at low latitudes. The magnetopause has been shown to oscillate with approximately the planetary rotation period due to compressive waves that originate in the near-planet region and propagate outward through the magnetospheric plasma (Clarke et al., 2006), and reconnection at the magnetopause has been observed (McAndrews et al., 2008), which could also affect the magnetopause position (Holzer and Slavin, 1978). Despite the large number of Cassini magnetopause crossings the topic of boundary waves on Saturn's magnetopause has not previously been investigated using Cassini observations; in this paper we present the first such study. We analysed a series of magnetopause crossings made on the dawn flank during a single spacecraft orbit in March 2006 to determine the boundary orientation. In the following sections we present evidence for boundary waves driven by the K–H instability during specific intervals. This result is relevant to our understanding of the transfer of solar wind momentum to the kronian magnetosphere, potentially the source location of Saturn kilometric radiation (Galopeau et al., 1995) and overall magnetospheric configuration.

2. Observations

The Cartesian coordinate system used throughout this study is the kronocentric solar magnetospheric (KSM) system which is Saturn-centred, with the positive x-axis pointing towards the Sun and the z-axis chosen such that the x–z plane contains Saturn's magnetic dipole axis, with the positive z-axis pointing north. The y-axis completes the orthogonal set, with the positive y-axis pointing towards dusk. The unit of distance used is Saturn radii (R_S; $1R_S = 60{,}268$ km).

To search for evidence of boundary waves we considered all the dawn flank magnetopause crossings made by Cassini between July 2004 (Saturn orbit insertion) and April 2006, since after this interval the spacecraft explored the magnetotail, staying mostly within the magnetosphere and rarely crossing the magnetopause. We inspected each spacecraft orbit, using the list of magnetopause crossings compiled by McAndrews (2007), to identify sets of multiple crossings that could be caused by boundary waves, and found a particular orbit during which more crossings occurred than any other. This orbit is referred to as Revolution (Rev) 22, using the mission nomenclature; panel a of Fig. 1 shows the spacecraft trajectory between 1 and 30 March 2006 in the x–y plane. This period encompasses part of the inbound pass of the Rev 22 orbit, during which Cassini stayed at low latitudes approximately in the plane of Saturn's rotational equator.

Panel b of Fig. 1 shows the x–y positions of the Rev 22 magnetopause crossings in more detail and illustrates that they can be grouped into three sets according to the days on which they occurred: set A (12 and 13 March), set B (14,15 and 16 March) and set C (17 March). Initially the crossings were grouped in this way because they naturally organise themselves into three groups according to their spatial locations, as shown in panel b. The projection of the Arridge et al. (2006) model of Saturn's magnetopause on the x–y plane is also shown in both panels of Fig. 1 for a typical solar wind dynamic pressure of 0.05 nPa (Crary et al., 2005; Masters et al., 2008), and reveals that Cassini was moving approximately parallel to the model surface during the interval spanning all the crossings.

The aim of our analysis of the Rev 22 crossings was to check for the presence of magnetopause boundary waves by using magnetic field data to determine the boundary normal at each crossing. To a first approximation, and in the absence of reconnection, the magnetopause is a tangential discontinuity (TD) separating the magnetised plasmas of the magnetosheath and magnetosphere—that is, there is no magnetic flux threading the boundary. In fact, the magnetopause is observed to have a finite thickness and consequently the normal to the magnetopause surface is usually given as the direction in which the field has a component equal to zero as the boundary (of finite extent) is crossed. As we will go on to discuss, calculating the normal to the boundary for each crossing required magnetic field measurements made by Cassini

Please cite this article as: Masters, A., et al., Surface waves on Saturn's dawn flank magnetopause driven by the Kelvin–Helmholtz instability. Planet. Space Sci. (2009), doi:10.1016/j.pss.2009.02.010

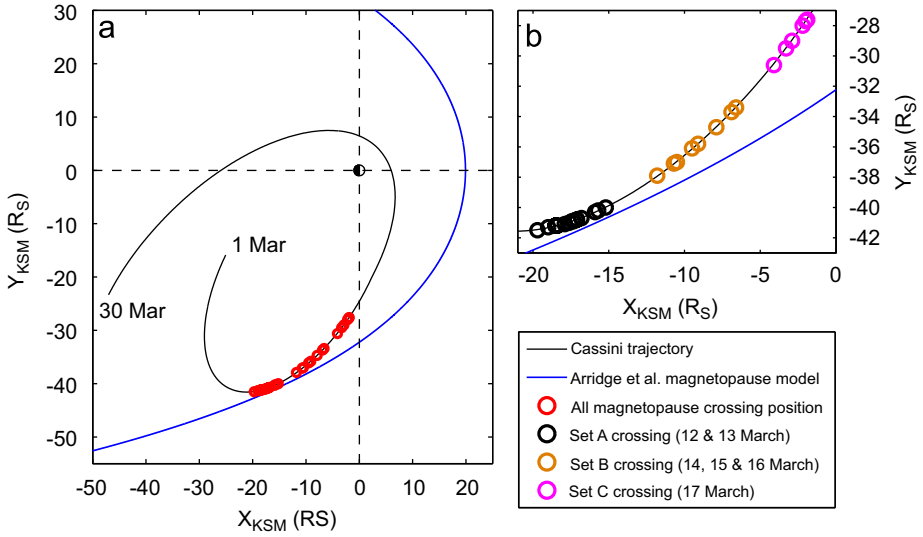

Fig. 1. Cassini's trajectory during March 2006 projected into the x–y plane. (a) Overview of the spacecraft trajectory for the whole month with all magnetopause crossings indicated. (b) Expanded view of the magnetopause crossings with crossing sets A, B and C indicated. In both plots the projection of the Arridge et al. (2006) magnetopause model is shown for a solar wind dynamic pressure of 0.05 nPa.

during the crossing, and so we were only able to include crossings with clear magnetic transitions in our analysis. We will now discuss the Rev 22 magnetopause crossings in more detail.

Fig. 2 presents the magnetic field and electron data for 12 and 13 March; the magnetic field data were acquired by the fluxgate magnetometer sensor (FGM) of the Cassini dual technique magnetometer (MAG) (Dougherty et al., 2004) at one-second resolution, and the electron data were taken by the electron spectrometer sensor (ELS) of the Cassini plasma spectrometer (CAPS) (Young et al., 2004) at 32-second resolution. In addition to the Cartesian KSM components of the magnetic field the spherical polar components are also shown. The field elevation angle (θ_B) is the angle between the field vector and the x–y plane, and the field azimuthal angle (φ_B) is the angle between the projection of the field vector into the x–y plane and the negative x direction (antisunward), with φ_B increasing in the direction of planetary rotation.

At the beginning of the interval shown in Fig. 2 Cassini was inside the magnetosphere; the magnetic field magnitude was ~2.3 nT, the electron number density was $\sim(2.4\times10^{-4})\,\mathrm{cm}^{-3}$ and the electron temperature was $\sim(4.9\times10^{6})\,\mathrm{K}$. Throughout the interval Cassini made excursions into a region of lower, more variable magnetic field, where the electron number density increased and the electron temperature decreased. In the first of these excursions the mean magnetic field magnitude was ~0.4 nT, the electron number density was $\sim9.8\times10^{-2}\,\mathrm{cm}^{-3}$ and the electron temperature was $\sim9.1\times10^{4}\,\mathrm{K}$. This distinctly different magnetic and electron environment corresponds to the magnetosheath, thus these are magnetosheath excursions bounded by magnetopause crossings. The time–energy spectrogram for electrons shown in panel f illustrates that in the magnetosphere the observed electron energy distribution lies mainly between ~100 and 1000 eV, whereas in the magnetosheath the electron energies lie between ~5 and 100 eV. Throughout the interval a population of spacecraft photoelectrons is present below 10 eV.

A magnetopause crossing can be identified as a relatively brief interval during which the strength and orientation of the field go from being magnetosphere-like to magnetosheath-like, or vice versa. During these intervals there was a distinct change in each of the KSM components of the field, this field re-orientation being well-illustrated by the field elevation and azimuthal angles (panels c and d of Fig. 2). The precise intervals corresponding to magnetopause crossings were identified and the resulting periods during which Cassini was in the magnetosheath proper are shaded in Fig. 2; in total 18 crossings were identified on 12 and 13 March and comprise the set A crossings. At this stage it is important to note that although the duration of the magnetosheath excursions was variable there are clearly two categories of excursion. The majority were of the order of hours, whereas four excursions were of the order of minutes and took place at ~13:03, ~13:41 and ~14:33 on 12 March and at ~02:17 on 13 March.

The presence of boundary layers adjacent to the kronian magnetopause has been previously confirmed (Lepping et al., 1981; McAndrews, 2007; McAndrews et al., 2008); in these regions the magnetic field and plasma properties are intermediate between those of the magnetosphere and magnetosheath, although the crossings of the magnetopause itself are still identifiable. During the interval shown in Fig. 2 signatures of boundary layers were observed on either side of a number of the crossings. In addition, at ~00:55 and ~08:24 on 12 March, and at ~01:27 on 13 March, Cassini observed an electron population with characteristics of both the typical magnetospheric and magnetosheath populations where the magnetic field did not undergo a clear transition between the two anticipated magnetic environments. As a result there were no clear magnetopause crossings either side of these encounters and thus we have interpreted them as boundary layer excursions. Since our analysis relies on magnetic field observations made during clear crossings of the magnetopause current layer we have not considered these encounters any further and they are not shown as shaded intervals in Fig. 2.

Following this inspection of the 12 and 13 March data sets we then considered the 14, 15 and 16 March data to identify the set B crossings. During this interval there were clear transitions between magnetospheric and magnetosheath electron populations; however, no clear re-orientation of the magnetic field was present. These are magnetopause crossings that correspond to a low magnetic shear which makes them untenable to our analysis, and as a result we were unable to include these set B crossings in our study of the boundary orientation.

The set C crossings that took place on 17 March had clearer signatures in the magnetic field data than the set B crossings. Fig. 3 presents the magnetic field and electron observations for

Please cite this article as: Masters, A., et al., Surface waves on Saturn's dawn flank magnetopause driven by the Kelvin–Helmholtz instability. Planet. Space Sci. (2009), doi:10.1016/j.pss.2009.02.010

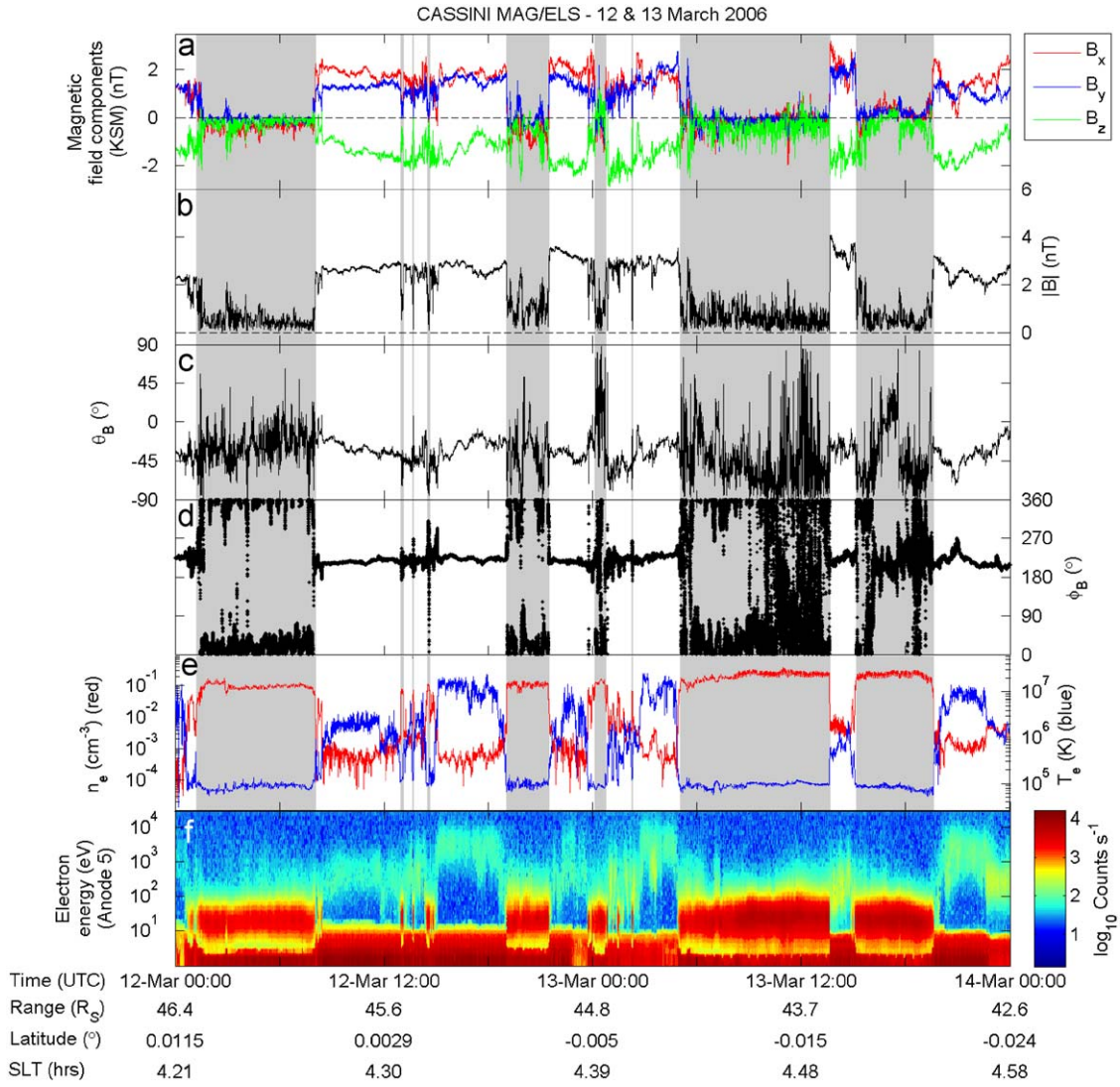

Fig. 2. MAG and ELS data for 12 and 13 March 2006 encompassing the set A magnetopause crossings. (a) Magnetic field components. (b) Magnetic field magnitude. (c) Field elevation angle. (d) Field azimuthal angle. (e) Electron number density and temperature. (f) Time–energy spectrogram of electron energy from ELS anode 5. Shaded intervals correspond to when the spacecraft was in the magnetosheath proper. The range, latitude and Saturn local time (SLT) of the spacecraft is shown under the plots.

17 March, using data from the same instruments, at the same time resolutions and in the same format as Fig. 2. At the beginning of 17 March Cassini was in the magnetosphere and as for the 12 and 13 March interval a number of excursions into the magnetosheath took place, where the field magnitude decreased, the field orientation changed and the measured electron population became colder and denser. The magnetopause crossings flanking each of these excursions were identified using the same criteria that was used to identify the set A crossings and resulted in six crossings that comprise set C. Once again, the shaded regions of Fig. 3 correspond to when Cassini was in the magnetosheath proper. At ~06:37 and ~14:52 there are boundary layer signatures, and between ~12:44 and ~13:48 and at ~20:20 there are boundary layer excursions. These features are similar to those seen on 12 and 13 March.

As discussed earlier in this section, the magnetopause surface normal direction for each crossing is the direction in which the field varies the least during the crossing transition. To determine this normal direction we carried out a minimum variance analysis (MVA) (Sonnerup and Scheible, 1998) of the high-resolution (32 vectors s^{-1}) magnetic field measurements that were made during each crossing by the FGM. This resulted in a magnetopause normal for each of the 18 crossings in set A and each of the six crossings in set C, in the following section we will discuss the implications of these normals for the dynamics of the boundary.

3. Boundary normal analysis

Carrying out MVA on a set of field vectors results in three unit vectors that form an orthogonal set: the directions of maximum, intermediate and minimum field variance. Each of these vectors is associated with an eigenvalue (λ_1, λ_2 and λ_3 for the maximum, intermediate and minimum variance directions, respectively) with the largest eigenvalue associated with the maximum variance direction and the smallest eigenvalue associated with the minimum variance direction (Sonnerup and Scheible, 1998). For our purposes we are only interested in the minimum variance direction produced by carrying out MVA on the field vectors corresponding to a magnetopause crossing as this is the boundary normal. The greater the ratio of λ_2–λ_3 the better defined the minimum variance direction is, thus this ratio indicates whether or not the magnetopause normal has been unambiguously identified.

Please cite this article as: Masters, A., et al., Surface waves on Saturn's dawn flank magnetopause driven by the Kelvin–Helmholtz instability. Planet. Space Sci. (2009), doi:10.1016/j.pss.2009.02.010

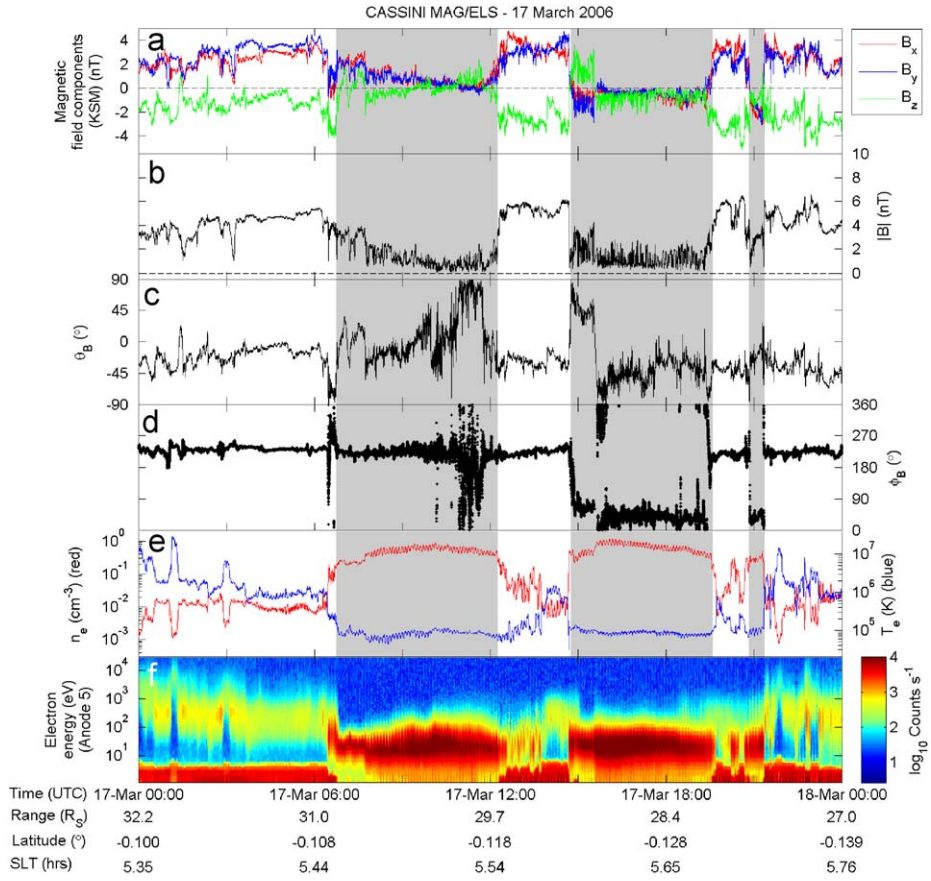

Fig. 3. MAG and ELS data for 17 March 2006 encompassing the set C magnetopause crossings. (a) Magnetic field components. (b) Magnetic field magnitude. (c) Field elevation angle. (d) Field azimuthal angle. (e) Electron number density and temperature. (f) Time–energy spectrogram of electron energy from ELS anode 5. Shaded intervals correspond to when the spacecraft was in the magnetosheath proper. The range, latitude and Saturn local time (SLT) of the spacecraft is shown under the plots.

The results of the MVA of the magnetopause crossings in sets A and C, including the surface normals, are given in Table 1. In addition to the time of each crossing the quantity λ_2/λ_3 is also given in the third column; the ratio is generally well above one which indicates that the normals are well-defined; however, for one crossing in set A the ratio was as low as 2.3. Analytical estimates of the angular error in the MVA normals (Khrabrov and Sonnerup, 1998) were all below 3°, the use of high-resolution magnetic field data was important in reducing the errors. The sixth, seventh and eighth columns of Table 1 give the x, y and z components of each MVA normal, respectively ($[N_x, N_y, N_z]$), all of the normals have been constrained to point out into the magnetosheath away from Saturn.

We then tested the normals based on an understanding of the physics of magnetopause crossings (Lepping and Burlaga, 1979). As the magnetopause TD is crossed the component of the field in the normal direction should be zero, thus the first test involved calculating the average field during each crossing interval and then determining the ratio of the component of the average field in the corresponding normal direction to the average field magnitude. The absolute value of this ratio for each crossing is given in the fourth column of Table 1 ($|B_N|/|B|$); Lepping and Behannon (1980) showed that for TDs this ratio should not be higher than 0.30. The highest value of this ratio for any crossing was 0.25, which suggests that we have correctly identified the normal in each case. To provide further confirmation of the validity of the normals we calculated the vector product of the average magnetic fields in one minute intervals immediately before and after each magnetopause crossing interval. Since no magnetic flux threads the surface of a TD, this vector product should also give the normal to each magnetopause crossing and can be compared to the normal determined using MVA (Knetter et al., 2004). The angular difference between the MVA normal and the vector product normal for each crossing is given in the fifth column of Table 1 (η), the maximum angular difference was 17.1° and the average error in these angular differences was 8.9°, due to the errors in the averaged field vectors used to calculate each vector product normal. As a result we concluded that the MVA and vector product normals are generally consistent, and thus the MVA normals are accurate representations of the boundary orientation.

The Arridge et al. (2006) model of Saturn's magnetopause was then scaled to intersect each crossing to predict the normal in each case. The angular difference between each MVA normal and its model normal counterpart was variable; however, the angle between the average MVA normal and the average model normal for sets A and C was 6.2° and 14.2°, respectively. This suggests that the average orientation of the boundary was in reasonably good agreement with the prediction of the Arridge et al. (2006) model for both crossing sets.

In the following discussion we will consider crossing sets A and C separately due to their spatial and temporal separation. By examining the behaviour of the normal direction for the set A crossings we identified a systematic flipping of the normals about the average of all the normals in a specific direction from each crossing to the next. To quantify the extent of the flipping we used the approach taken by Lepping and Burlaga (1979) in their analysis of crossings of Earth's magnetopause, where they also observed flipping normals. We carried out MVA on the set A normals to calculate the maximum variance direction, since this is

Please cite this article as: Masters, A., et al., Surface waves on Saturn's dawn flank magnetopause driven by the Kelvin–Helmholtz instability. Planet. Space Sci. (2009), doi:10.1016/j.pss.2009.02.010

Table 1
Boundary normals for the magnetopause crossings in sets A and C.

Day of month	Time (UTC)	λ_2/λ_3	$\lvert B_N\rvert/\lvert B\rvert$	η (deg.)	N_x	N_y	N_z	α (deg.)	β (deg.)
12	01:14:28	11.4	0.03	11.1	0.51	−0.81	−0.29	6.4	−1.2
12	08:03:56	6.8	0.25	15.0	0.45	−0.81	−0.38	8.9	4.6
12	12:58:37	5.6	0.03	10.7	0.73	−0.58	0.37	−10.9	−41.5
12	13:07:39	26.6	0.01	1.3	−0.05	−0.88	−0.47	−5.3	31.7
12	13:39:56	3.8	0.17	15.3	0.35	−0.94	−0.01	−13.3	−3.2
12	13:42:37	25.5	0.10	14.9	−0.13	−0.84	−0.52	−4.5	37.5
12	14:29:29	2.3	0.02	15.6	0.70	−0.72	0.01	2.0	−21.8
12	14:37:36	6.3	0.01	3.5	0.13	−0.89	−0.44	−0.6	21.8
12	19:02:24	4.9	0.06	13.0	0.68	−0.68	−0.27	14.6	−11.2
12	21:30:00	24.0	0.06	2.7	0.34	−0.85	−0.41	5.8	11.2
13	00:08:27	17.0	0.02	3.1	0.64	−0.74	0.19	−8.8	−26.8
13	00:45:22	7.6	0.04	9.9	0.07	−0.93	−0.35	−7.9	21.9
13	02:15:01	8.3	0.11	10.6	0.72	−0.65	0.23	−5.4	−33.0
13	02:18:03	6.6	0.03	7.6	0.83	−0.07	0.55	0.9	−72.1
13	05:02:03	15.0	0.05	9.3	−0.52	−0.50	−0.69	0.9	69.1
13	13:39:08	57.9	0.10	13.5	0.35	−0.83	−0.42	7.0	10.9
13	15:09:33	10.7	0.03	6.3	0.77	−0.64	−0.03	8.8	−24.7
13	19:37:30	24.7	0.08	13.9	0.10	−0.90	−0.41	−3.1	22.3
17	06:44:50	7.8	0.05	10.3	0.69	−0.72	−0.13	2.0	−13.8
17	12:15:13	3.5	0.17	16.9	0.30	−0.84	−0.46	1.1	16.4
17	14:45:21	5.0	0.16	3.9	0.72	−0.65	−0.22	8.8	−12.8
17	19:34:25	9.9	0.16	12.6	0.33	−0.86	−0.39	−1.3	12.6
17	20:51:15	6.8	0.08	11.3	0.63	−0.78	0.05	−9.3	−17.9
17	21:21:11	6.7	0.10	17.1	0.29	−0.86	−0.42	−1.5	15.2

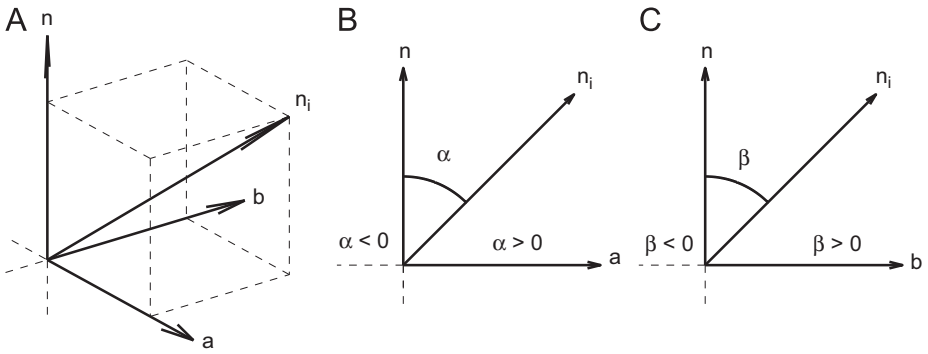

Fig. 4. Diagrams illustrating how the angles α and β were defined for each MVA normal. n_i is an arbitrary MVA normal, n is the average of the MVA normals, b is the flipping direction of the normals, and a is the direction perpendicular to the flipping direction. (A) Three-dimensional view showing the orientation of the vectors. (B) Projection of the vectors into the n–a plane, showing the definition of the angle α. (C) Projection of the vectors into the n–b plane, showing the definition of the angle β.

the direction in which the flipping about the average normal occurs, and obtained a ratio of λ_1–λ_2 of 6.2, which implies that the direction in which the normals oscillate is reasonably well-defined.

This flipping direction (hereafter referred to as 'vector b') had a positive x component and made an angle of ~88° with the average of all the normals (hereafter referred to as 'vector n'). Vector b was rotated by ~2° in the n–b plane so that it was perpendicular to vector n. We then took the vector product of vectors b and n to define a direction perpendicular to the flipping direction (hereafter referred to as 'vector a'). To quantify the flipping of the normals two angles were then defined and calculated for each normal: α and β. α is the angular difference between vector n and the projection of each normal into the plane containing vectors a and n, with positive α corresponding to a positive projection of the normal onto vector a, and vice versa. Whereas β is the angular difference between vector n and the projection of each normal into the plane containing vectors b and n; positive β corresponds to a positive projection of the normal onto vector b, and vice versa. Thus α and β describe how each normal differs from the average normal in the direction perpendicular and parallel to the direction of the flipping, respectively. The diagrams shown in Fig. 4 illustrate how these two angles were defined for each normal.

The values of α and β for each crossing in set A are shown in the ninth and tenth columns of Table 1; for these crossings α ranges from −13.3° to 14.6° and there is no systematic behaviour of the angle. However, the β angle reveals the extent of the flipping implied by the initial visual inspection; there is a clear oscillation between positive and negative values of β for the first 13 of the 18 crossings in the set, with β ranging from −41.5° to 37.5°. This flipping effect cannot be explained by purely normal oscillations of the surface and is clear evidence that regular boundary waves led to these crossings (Lepping and Burlaga, 1979). The fact that the flipping direction has a positive x component, the first value of β is positive, and that first crossing in set A was from the magnetosphere to the magnetosheath, suggests that the waves were propagating tailward.

The normals indicate that boundary waves not only caused the excursions that lasted for the order of hours, but also the shorter excursions of the order of minutes that were observed during set A, and were mentioned in the previous section. This implies that during the set A interval two types of boundary wave were present that had different periods. The longer magnetosheath

Please cite this article as: Masters, A., et al., Surface waves on Saturn's dawn flank magnetopause driven by the Kelvin–Helmholtz instability. Planet. Space Sci. (2009), doi:10.1016/j.pss.2009.02.010

excursions due to the longer period waves had a variable duration (as shown in Figs. 2 and 3), which was possibly caused by normal motions of the boundary leading to Cassini encountering a different part of the waveform from one crossing to the next. However the set of three excursions in set A, that all occurred within one hour of 14:00 on 12 March 2006, which were caused by the shorter period waves, have a more consistent duration. To calculate the period of these shorter period waves we assumed that the start of each of the three excursions corresponded to Cassini encountering the same part of the waveform, and the same for the end of each excursion, and that the waveform was not subject to temporal variation. Thus, we took the time duration between the start (end) of an excursion and the start (end) of the following excursion as the period of the waves. This left us with four time durations; we calculated the average and standard deviation of this set to give the period of the waves, and the associated error, respectively. The resulting period of the shorter period waves was 45 ± 9 min, which is longer than the 23 ± 2 min period of the boundary waves identified by Lepping et al. (1981) using Voyager 1 observations. The boundary layer excursions noted in the previous section could also be due to these shorter period waves.

For crossings 14–18 of set A the positive–negative oscillation of β breaks down, indicating that there are no longer waves on the magnetopause during the interval spanning these crossings. However, we note that these normals still approximately lie in the plane in which the previous normals were flipping, and that the fourteenth and fifteenth crossing normals made angles of 72.3° and 68.9° to the average normal, respectively. We therefore conclude that the orientation of the magnetopause during these last five crossings was intimately related to the preceding boundary waves and that the magnetopause had a highly perturbed orientation at the time of two of the crossings.

The set C crossings were then considered and once again a visual inspection suggested that the normals flipped in a preferred direction, so the same approach was used to examine the oscillation of the set C crossing normals. MVA of the set C normals led to a well-defined maximum variance direction, with a λ_1–λ_2 ratio of 8.0, that was then used to define α and β in exactly the same way as for set A. The values of α and β for the set C normals, shown in Table 1, lead to the same conclusion as for set A; the crossings were caused by regular boundary waves propagating tailward along the magnetopause surface. As a test for our identification of boundary waves during the set A and set C crossings we also examined the vector product normals for the crossings that were mentioned earlier. The same behaviour of the normals was observed and the quantitative results were very similar, providing confirmation of the identification of boundary waves.

In order to investigate the direction of propagation of these waves in more detail we began by comparing the flipping directions for the set A and set C normals and found that the angular difference between the two was 0.6°, which suggests that the set A and set C crossings were both caused by the same type of wave activity. To further examine the wave propagation direction we used the approach described by Huddleston et al. (1997), which uses each pair of consecutive normals to infer a wave propagation direction. Thus 17 propagation directions were calculated for the set A crossings and 5 were calculated for the set C crossings; Fig. 5 presents the propagation directions projected onto the x–y and x–z planes for each set. The projection of the crossing positions onto the x–z plane appear to lie further from the typical position of the magnetopause than their projection onto the x–y plane because the crossings took place at low latitudes in the pre-dawn sector. There is little spread in both sets of propagation directions compared to when this approach has been used in previous studies of planetary magnetopause boundary waves (Huddleston et al., 1997) and the similarity of the propagation directions in both sets is apparent. Panels a and c of Fig. 5 show that the boundary wave propagation directions are approximately parallel to the Arridge et al. (2006) model of the magnetopause, whereas panels b and d reveal that the waves do not propagate strictly in the anti-sunward direction. The waves propagated tailward along the directions shown.

As defined in Section 2, in the KSM coordinate system the x–z plane contains the sunward direction (the positive x-axis) and Saturn's magnetic dipole vector; however, the dipole vector is not coincident with the z-axis. During the period of the Rev 22 orbit the planet's dipole axis was tilted 18.3° antisunward of the z-axis, and since Saturn's magnetic dipole and rotation axes are the same to within 1° (e.g. Smith et al., 1980) the average direction of wave propagation for sets A and C is within 24° of Saturn's magnetic and rotational equators. We considered calculating the properties of the boundary waves using each set of three consecutive normals using the analytical approach of Lepping and Burlaga (1979); however, Cassini's trajectory during Rev 22 was not appropriate for the use of this technique as the spacecraft had a small velocity component in the direction normal to the boundary, prohibiting the accurate determination of the spatial and temporal characteristics of the waves.

4. Discussion

We have identified tailward propagating surface waves on Saturn's dawn flank magnetopause during the Rev 22 orbit. What driving mechanism generates these waves? Fluctuations in the dynamic pressure of the solar wind can generate boundary waves on a planet's magnetopause (Sibeck, 1990); however, this external driver is implausible because of the wave propagation directions shown in Fig. 5. This potential driving mechanism cannot provide a clear explanation of the north–south component of the wave propagation directions, since waves due to such pressure fluctuations typically propagate tailward, away from the nose of the magnetopause, in the direction of the magnetosheath flow.

Another candidate mechanism is the oscillations of Saturn's magnetopause that were identified and discussed by Clarke et al. (2006). They showed that the magnetopause oscillates at approximately Saturn's rotation period with an estimated amplitude of $\sim 2R_S$, and proposed that this is due to compressive waves that originate from a corotating source in the near-planet region. In their identification they used Cassini magnetopause crossings from two orbits (Rev 16 and Rev 17) and did not investigate the possibility that the orientation of the boundary was perturbed by this oscillation. They proposed that the nature of the oscillation is a relatively large 'bulge' which propagates along the magnetopause in the direction of planetary rotation as a result of the compressive wave fronts. If this effect perturbs the boundary orientation we would expect the resultant flipping of the normals to imply sunward, rather than tailward, propagation on the dawn flank; this is not the case for the Rev 22 boundary waves. In addition the magnetosheath excursion times during Rev 22 are variable and are not organised by the approximate planetary rotation period, thus we ruled out this possible driving mechanism.

As mentioned in Section 1, it has been proposed that magnetopause boundary waves can be driven by reconnection-related phenomena. For the case of Earth's magnetopause, Song et al. (1988) showed that for a southward orientation of the IMF the boundary became more oscillatory. They suggested that dayside reconnection associated with southward IMF leads to surface waves that propagate tailward, away from the subsolar

Please cite this article as: Masters, A., et al., Surface waves on Saturn's dawn flank magnetopause driven by the Kelvin–Helmholtz instability. Planet. Space Sci. (2009), doi:10.1016/j.pss.2009.02.010

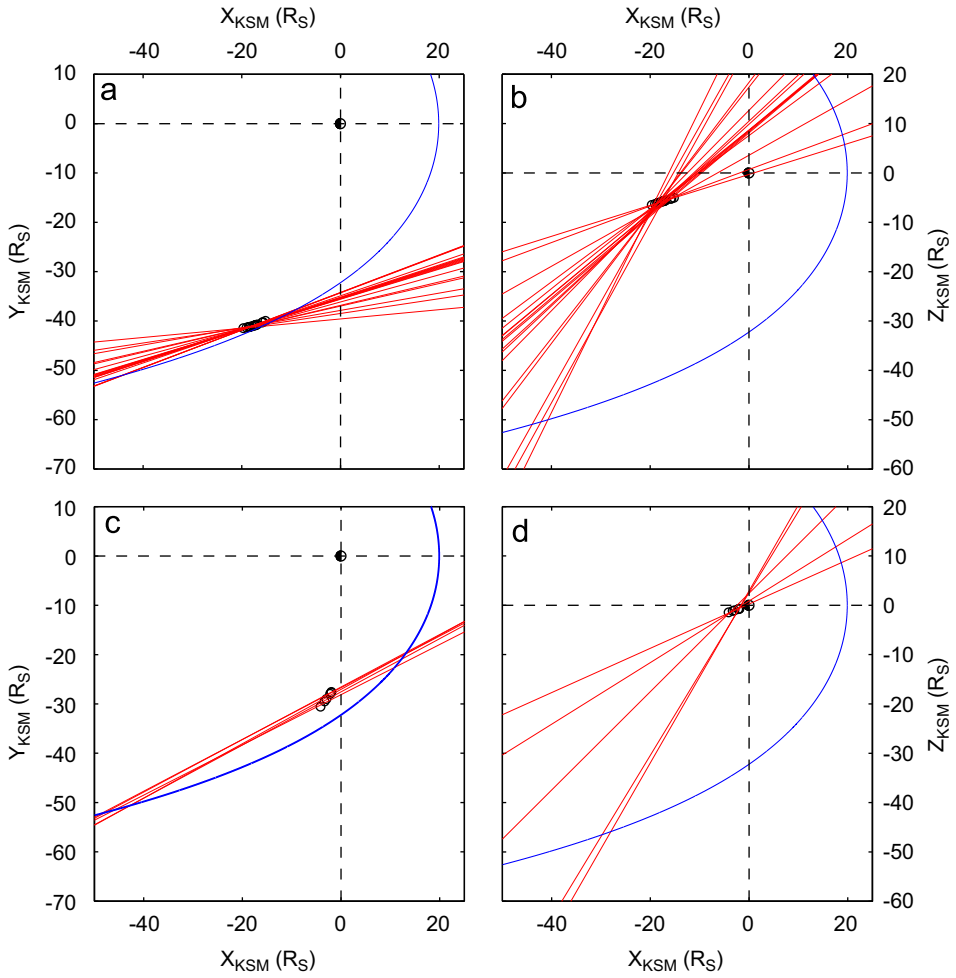

Fig. 5. Boundary wave propagation directions. All propagation directions are shown as red lines. (a) Set A directions in the *x*–*y* plane. (b) Set A directions in the *x*–*z* plane. (c) Set C directions in the *x*–*y* plane. (d) Set C directions in the *x*–*z* plane. In all plots the projection of the Arridge et al. (2006) magnetopause model is shown in blue for a solar wind dynamic pressure of 0.05 nPa. (For interpretation of the references to colour in this figure legend, the reader is referred to the web version of this article.)

point. However, although reconnection has been observed at Saturn's dayside magnetopause (McAndrews et al., 2008), no examples of kronian FTEs have been reported to date; thus, it is possible that the nature of dayside reconnection at Saturn differs from the terrestrial case, making it unclear whether reconnection-related phenomena can produce boundary waves on Saturn's magnetopause. In addition, a reconnection-related driving mechanism cannot provide a clear explanation of the north–south component of the wave propagation directions.

As also discussed in Section 1, it has been hypothesised that Saturn's dawn flank magnetopause is unstable to the growth of the K–H instability, which should result in boundary waves. In order to assess whether the waves identified during Rev 22 were K–H driven we considered the K–H instability criterion given in Eq. (1) (e.g. Ogilvie and Fitzenreiter, 1989), where $\boldsymbol{k}$ is the wave vector, $\boldsymbol{V}$ is the flow velocity, μ_0 is the permeability of free space, ρ is the mass density, $\boldsymbol{B}$ is the magnetic field vector, and the subscripts 1 and 2 indicate whether a parameter corresponds to the magnetosheath or magnetosphere, respectively.

$$[\boldsymbol{k}\cdot(\boldsymbol{V}_2-\boldsymbol{V}_1)]^2 > \frac{1}{\mu_0}\left(\frac{1}{\rho_1}+\frac{1}{\rho_2}\right)[(\boldsymbol{k}\cdot\boldsymbol{B}_1)^2+(\boldsymbol{k}\cdot\boldsymbol{B}_2)^2] \quad (1)$$

It is clear that magnetic tension force acts to stabilise the boundary (Southwood, 1968) whereas a strong flow velocity shear makes the interface more likely to become K–H unstable. Pu and Kivelson (1984) have already investigated the stability of the kronian magnetopause boundary from a theoretical perspective; however, a qualitative consideration of Eq. (1) is important in identifying the driving mechanism generating the Rev 22 surface waves. We also note that the boundary waves may have been generated by the growth of the K–H instability at a part of the interface other than the region in which they were observed, with the waves subsequently propagating to the region of observation, but nonetheless it is potentially important to consider the parameters measured where the waves were observed. Kivelson and Pu (1984) discussed that if the field magnitude either side of the interface differs greatly then the most unstable wave vector is roughly perpendicular to the stronger of the two fields, since the stronger field exerts a greater magnetic tension force. During the intervals of both the set A and set C crossings of Rev 22 the magnetospheric field was stronger than the magnetosheath field (as shown in Figs. 2 and 3). If we take the direction in which the normals flip for each set as the unstable wave vector direction, then the angular difference between the wave vector and the magnetospheric field was 79.3° and 69.2°, respectively. Given that both of the stronger magnetospheric fields are within 21° of being perpendicular to the appropriate wave vector, that a strong flow velocity shear is expected at the dawn flank of the boundary, and that the average wave propagation direction for both the set A and set C crossings is within 24° of Saturn's rotational equator, a K–H instability driving mechanism is plausible, since it is able to clearly explain the wave propagation directions. As this is by far

Please cite this article as: Masters, A., et al., Surface waves on Saturn's dawn flank magnetopause driven by the Kelvin–Helmholtz instability. Planet. Space Sci. (2009), doi:10.1016/j.pss.2009.02.010

the most plausible mechanism for generating the observed waves, we conclude that the Rev 22 surface waves were driven by the K–H instability.

Our analysis of the Rev 22 magnetopause crossings has revealed two types of wave activity: waves with a period of the order of hours that we were unable to accurately constrain, and waves with a period of 45 ± 9 min. It is possible that the shorter period wave activity is similar to that observed by Voyager 1 (Lepping et al., 1981), although we obtain a longer average period. Since we see numerous excursions caused by the longer period waves and only three caused by the shorter period waves this suggests that either the shorter period waves were a transient feature of the wave activity, or they had an amplitude that was less than that of the longer period waves and were present throughout the set A and set C intervals. Since we observe a number of excursions into the boundary layer with durations of the order of minutes in both sets A and C we propose that these shorter period waves were present throughout the set A and set C intervals and resulted in these features.

The qualitative picture of the nature of the wave activity on the dawn flank magnetopause during the intervals of the set A and set C crossings of Rev 22 that we propose is shown in Fig. 6. The schematic illustrates that we suggest that smaller amplitude, shorter period waves were superposed with larger amplitude, longer period waves on the magnetopause boundary. Many of the initial, theoretical studies of the K–H instability at a planetary magnetopause assumed that the plasmas on either side of the interface were incompressible (e.g. Sen, 1963); Pu and Kivelson (1983a) then showed that for compressible plasmas two kinds of dominant surface wave can exist simultaneously. They labelled these waves fast and slow waves because of their different propagation speeds. We note that the two types of wave activity we have identified on Saturn's magnetopause during Rev 22 may be examples of these two types of K–H surface wave; however, since we are unable to accurately determine all of the properties of each type of wave we are unable to investigate this further.

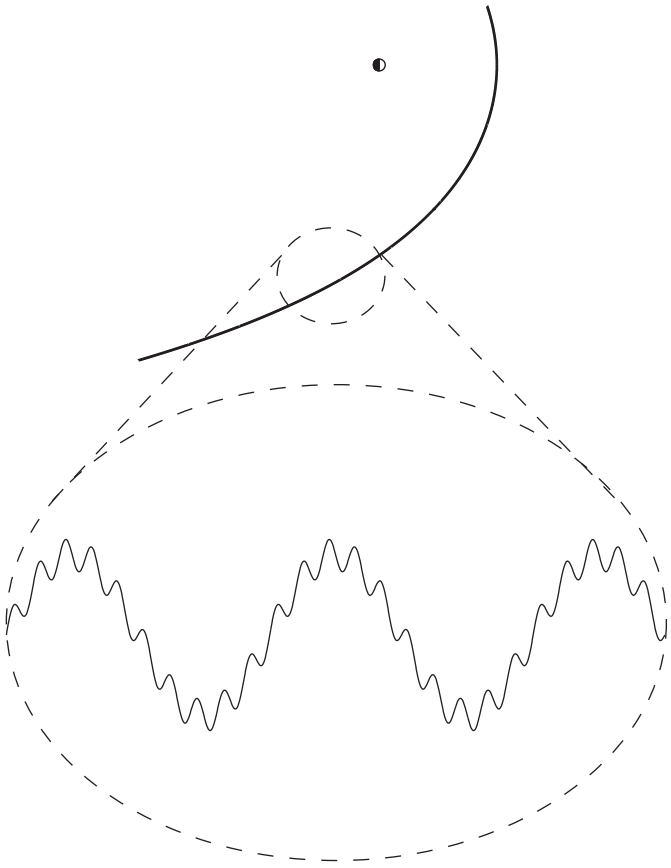

Fig. 6. Schematic illustrating the proposed nature of the wave activity present on Saturn's dawn flank magnetopause at the time of the crossings in sets A and C. Solid lines represent the magnetopause boundary, dashed lines represent an expanded view of the part of the boundary observed during the Rev 22 orbit.

5. Conclusions

In this paper we have examined the orientation of Saturn's dawn flank magnetopause surface by analysing a series of magnetopause crossings made by the Cassini spacecraft in March 2006. The normal to the boundary was calculated for each crossing using MVA and the resulting series of normals revealed that regular surface waves were present on the magnetopause during both intervals analysed. Two categories of surface wave were identified, both of which were propagating tailward in a direction that was within 24° of Saturn's magnetic and rotational equators. We conclude that these surface waves were driven by the K–H instability, and we propose that during the intervals considered a superposition of two types of boundary wave activity was present.

This result contributes to our understanding of the nature of the perturbations of Saturn's magnetopause, and thus the overall configuration of Saturn's magnetosphere. If the growth of the K–H instability leads to significant boundary perturbations then this has implications for the transport of solar wind energy into the magnetosphere, since deformations of the magnetopause can launch compressive waves into the magnetosphere and can lead to field-aligned current systems (e.g. Sibeck, 1990). The anticipated dawn–dusk asymmetry in the K–H stability of Saturn's magnetopause may also have implications for the source locations of Saturn kilometric radiation auroral emissions (Galopeau et al., 1995). For these reasons the topic of Kelvin–Helmholtz instability at Saturn's magnetopause is deserving of further research.

Cassini has made a number of crossings of Saturn's dawn flank magnetopause, in addition to those discussed in this study. The analysis of further crossings from different spacecraft orbits is necessary to build up a clearer picture of the dynamics of the magnetopause, in particular a detailed survey of the dawn flank crossings could reveal how often the boundary is unstable to the growth of surface waves. The simulations of Fukazawa et al. (2007) suggest that rolled-up vortices can form near the nose of Saturn's magnetopause, before propagating tailward along the dawn flank. The identification of such structures is an important topic of further study.

Acknowledgements

AM acknowledges useful discussions with K. Nykyri, M.G. Kivelson and the support of the Royal Astronomical Society. We acknowledge the support of the MAG data processing/distribution staff and L.K. Gilbert and G.R. Lewis for ELS data processing. This work was supported by UK STFC through the award of a studentship (AM) and research grants to MSSL/UCL and Imperial College London.

References

Acuña, M.H., Ness, N.F., 1980. The magnetic field of Saturn—Pioneer 11 observations. Science 207, 444–446.

Arridge, C.S., Achilleos, N., Dougherty, M.K., Khurana, K.K., Russell, C.T., 2006. Modeling the size and shape of Saturn's magnetopause with variable dynamic pressure. J. Geophys. Res. 111 (A11227).

Aubry, M.P., Kivelson, M.G., Russell, C.T., 1971. Motion and structure of the magnetopause. J. Geophys. Res. 76, 1673–1696.

Chapman, S., Ferraro, V.C.A., 1931. A new theory of magnetic storms. J. Geophys. Res. 36, 171–186.

Chen, S.-H., Kivelson, M.G., 1993. On nonsinusoidal waves at the Earth's magnetopause. Geophys. Res. Lett. 20, 2699–2702.

Clarke, K.E., André, N., Andrews, D.J., Coates, A.J., Cowley, S.W.H., Dougherty, M.K., Lewis, G.R., McAndrews, H.J., Nichols, J.D., Robinson, T.R., Wright, D.M., 2006. Cassini observations of planetary-period oscillations of Saturn's magnetopause. Geophys. Res. Lett. 33, L23104.

de Keyser, J., Dunlop, M.W., Owen, C.J., Sonnerup, B.U.Ö., Haaland, S.E., Vaivads, A., Paschmann, G., Lundin, R., Rezeau, L., 2005. Magnetopause and boundary layer. Space Sci. Rev. 118, 231–320.

Crary, F.J., Clarke, J.T., Dougherty, M.K., Hanlon, P.G., Hansen, K.C., Steinberg, J.T., Barraclough, B.L., Coates, A.J., Gérard, J.-C., Grodent, D., Kurth, W.S., Mitchell, D.G., Rymer, A.M., Young, D.T., 2005. Solar wind dynamic pressure and electric field as the main factors controlling Saturn's aurorae. Nature 433, 720–722.

Dougherty, M.K., Kellock, S., Southwood, D.J., Balogh, A., Smith, E.J., Tsurutani, B.T., Gerlach, B., Glassmeier, K.-H., Gleim, F., Russell, C.T., Erdos, G., Neubauer, F.M., Cowley, S.W.H., 2004. The Cassini magnetic field investigation. Space Sci. Rev. 114, 331–383.

Dungey, J.W., 1955. Electrodynamics of the outer atmosphere. In: Proceedings of the Ionosphere Conference. The Physical Society of London.

Dungey, J.W., 1961. Interplanetary magnetic field and the auroral zones. Phys. Rev. Lett. 6, 47–48.

Eviatar, A., Richardson, J.D., 1986. Corotation of the kronian magnetosphere. J. Geophys. Res. 91, 3299–3303.

Fairfield, D.H., Otto, A., Mukai, T., Kokubun, S., Lepping, R.P., Steinberg, J.T., Lazarus, A.J., Yamamoto, T., 2000. Geotail observations of the Kelvin–Helmholtz instability at the equatorial magnetotail boundary for parallel northward fields. J. Geophys. Res. 105, 21159–21174.

Fejer, J.A., 1964. Hydromagnetic stability at a fluid velocity discontinuity between compressible fluids. Phys. Fluids 7, 499–503.

Fukazawa, K., Ogino, T., Walker, R.J., 2007. Vortex-associated reconnection for northward IMF in the kronian magnetosphere. Geophys. Res. Lett. 34, L23201.

Galopeau, P.H.M., Zarka, P., Le Quéau, D., 1995. Source location of Saturn's kilometric radiation: the Kelvin–Helmholtz instability hypothesis. J. Geophys. Res. 100, 26397–26410.

Hasegawa, H., Fujimoto, M., Phan, T.-D., Rème, H., Balogh, A., Dunlop, M.W., Hashimoto, C., TamDokoro, R., 2004. Transport of solar wind into Earth's magnetosphere through rolled-up Kelvin–Helmholtz vortices. Nature 430, 755–758.

Holzer, R.E., Slavin, J.A., 1978. Magnetic flux transfer associated with expansions and contractions of the dayside magnetosphere. J. Geophys. Res. 83, 3831–3839.

Huddleston, D.E., Russell, C.T., Le, G., 1997. Magnetopause structure and the role of reconnection at the outer planets. J. Geophys. Res. 102, 24289–24302.

Khrabrov, A.V., Sonnerup, B.U.Ö., 1998. Error estimates for minimum variance analysis. J. Geophys. Res. 103, 6641–6652.

Kivelson, M.G., Pu, Z.-Y., 1984. The Kelvin–Helmholtz instability on the magnetopause. Planet. Space Sci. 32, 1335–1341.

Knetter, T., Neubauer, F.M., Horbury, T., Balogh, A., 2004. Four-point discontinuity observations using cluster magnetic field data: a statistical survey. J. Geophys. Res. 109 (A06102).

Lepping, R.P., Burlaga, L.F., 1979. Geomagnetopause surface fluctuations observed by Voyager 1. J. Geophys. Res. 84, 7099–7106.

Lepping, R.P., Behannon, K.W., 1980. Magnetic field directional discontinuities. I—minimum variance errors. J. Geophys. Res. 85, 4695–4703.

Lepping, R.P., Burlaga, L.F., Klein, L.W., 1981. Surface waves on Saturn's magnetopause. Nature 292, 750–753.

Lepping, R.P., 1992. Magnetic boundaries of the outer planets—a review. Adv. Space Res. 12, 25–42.

Masters, A., Achilleos, N., Dougherty, M.K., Slavin, J.A., Hospodarsky, G.B., Arridge, C.S., Coates, A.J., 2008. An empirical model of Saturn's bow shock: Cassini observations of shock location and shape. J. Geophys. Res. 113 (A10210).

McAndrews, H.J., 2007. Cassini observations of low energy electrons in and around Saturn's magnetosphere. PhD thesis. University of London.

McAndrews, H.J., Owen, C.J., Thomsen, M.F., Lavraud, B., Coates, A.J., Dougherty, M.K., Young, D.T., 2008. Evidence for reconnection at Saturn's magnetopause. J. Geophys. Res. 113 (A04210).

Nikutowski, B., Büchner, J., Otto, A., Kistler, L.M., Korth, A., Moukis, C., Haerendel, G., Baumjohann, W., 2002. Equator-S observation of reconnection coupled to surface waves. Adv. Space Res. 29, 1129–1134.

Nykyri, K., Otto, A., 2001. Plasma transport at the magnetospheric boundary due to reconnection in Kelvin–Helmholtz vortices. Geophys. Res. Lett. 28, 3565–3568.

Nykyri, K., Otto, A., 2004. Influence of the hall term on KH instability and reconnection inside KH vortices. Ann. Geophys. 22, 935–949.

Nykyri, K., Otto, A., Lavraud, B., Mouikis, C., Kistler, L.M., Balogh, A., Rème, H., 2006. Cluster observations of reconnection due to the Kelvin–Helmholtz instability at the dawnside magnetospheric flank. Ann. Geophys. 24, 2619–2643.

Ogilvie, K.W., Fitzenreiter, R.J., 1989. The Kelvin–Helmholtz instability at the magnetopause and inner boundary layer surface. J. Geophys. Res. 94, 15113–15123.

Pu, Z.-Y., Kivelson, M.G., 1983a. Kelvin–Helmholtz instability at the magnetopause. I—solution for compressible plasmas. II—energy flux into the magnetosphere. J. Geophys. Res. 88, 841–861.

Pu, Z.-Y., Kivelson, M.G., 1983b. Kelvin–Helmholtz instability at the magnetopause: energy flux into the magnetosphere. J. Geophys. Res. 88, 853–862.

Pu, Z.-Y., Kivelson, M.G., 1984. Kelvin–Helmholtz instability and MHD surface waves on Saturn's magnetopause. Chin. J. Space Sci. 4, 105–111.

Russell, C.T., Elphic, R.C., 1978. Initial ISEE magnetometer results—magnetopause observations. Space Sci. Rev. 22, 681–715.

Russell, C.T., Elphic, R.C., 1979. ISEE observations of flux transfer events at the dayside magnetopause. Geophys. Res. Lett. 6, 33–36.

Sen, A.K., 1963. Stability of hydromagnetic Kelvin–Helmholtz discontinuity. Phys. Fluids 6, 1154–1163.

Sen, A.K., 1965. Stability of the magnetospheric boundary. Planet. Space Sci. 13, 131.

Seon, J., Frank, L.A., Lazarus, A.J., Lepping, R.P., 1995. Surface waves on the tailward flanks of the Earth's magnetopause. J. Geophys. Res. 100, 11907–11922.

Sibeck, D.G., 1990. A model for the transient magnetospheric response to sudden solar wind dynamic pressure variations. J. Geophys. Res. 95, 3755–3771.

Sibeck, D.G., Lopez, R.E., Roelof, E.C., 1991. Solar wind control of the magnetopause shape, location, and motion. J. Geophys. Res. 96, 5489–5495.

Smith, E.J., Davis, L., Jones, D.E., Coleman, P.J., Colburn, D.S., Dyal, P., Sonett, C.P., 1980. Saturn's magnetic field and magnetosphere. Science 207, 407–410.

Song, P., Elphic, R.C., Russell, C.T., 1988. ISEE 1 and 2 observation of the oscillating magnetopause. Geophys. Res. Lett. 15, 744–747.

Sonnerup, B.U.Ö., Schreible, M., 1998. Minimum and maximum variance analysis. In: Paschmann, G., Daly, P.W. (Ed.), Analysis methods for multi-spacecraft data.

Southwood, D.J., 1968. The hydromagnetic stability of the magnetospheric boundary. Planet. Space Sci. 16, 587.

Stone, E.C., Miner, E.D., 1981. Voyager 1 encounter with the Saturnian system. Science 212, 159–163.

Stone, E.C., Miner, E.D., 1982. Voyager 2 encounter with the Saturnian system. Science 215, 499–504.

Young, D.T., et al., 2004. Cassini plasma spectrometer investigation. Space Sci. Rev. 114, 1–112.

Please cite this article as: Masters, A., et al., Surface waves on Saturn's dawn flank magnetopause driven by the Kelvin–Helmholtz instability. Planet. Space Sci. (2009), doi:10.1016/j.pss.2009.02.010